Sterile neutrino dark matter production in lepton asymmetric universe and its observational implications

Kentaro Kasai (ICRR, The University of Tokyo)
Mainly based on arXiv:2402.11902 (JCAP published)

Collaboration with :
Masahiro Kawasaki (ICRR, The University of Tokyo)
Kai Murai (Tohoku University)

KMI Theory seminar 2025/6/17

Self-introduction

Kentaro Kasai, Ph. D. Student in ICRR
Supervisor : Kawasaki-san (ICRR)

Main interest : early-universe cosmology

Study 1. Formation model of “primordial black holes”

arXiv:2205.10148 (JCAP)
arXiv:2305.13023 (JCAP)
arXiv:2310.13333 (JCAP)
arXiv: 2412.09790 (PR. D)

Study 2. Sterile neutrino dark matter, leptogenesis

arXiv:2402.11902 “Affleck-Dine leptogenesis scenario
For resonant production of sterile neutrino dark matter” (JCAP)

Study 3. Primordial gravitational waves (Stochastic GW background)

arXiv: 2412.17912 (On the GWs from cosmological FOPT)

Self-introduction

Kentaro Kasai, Ph. D. Student in ICRR
Supervisor : Kawasaki-san (ICRR)

Main interest : early-universe cosmology

Study 1. Formation model of “primordial black holes”

arXiv:2205.10148 (JCAP)
arXiv:2305.13023 (JCAP)
arXiv:2310.13333 (JCAP)
arXiv: 2412.09790 (PR. D)

Study 2. Sterile neutrino dark matter, leptogenesis

arXiv:2402.11902 “Affleck-Dine leptogenesis scenario
For resonant production of sterile neutrino dark matter” (JCAP) ← **Today**

Study 3. Primordial gravitational waves (Stochastic GW background)

arXiv: 2412.17912 (On the GWs from cosmological FOPT)

Today's talk :

Phenomenology with the
"large" primordial neutrino/anti-neutrino asymmetry

$$(n_\nu - n_{\bar{\nu}})/s_{\rm tot} \gtrsim \mathcal{O}(10^{-4}) \gg n_B/s_{\rm tot}$$

- **Implications:**

1. Can assist resonant production of sterile neutrino DM
   → Comprehensive discussion of the allowed parameter region

X. D. Shi, G. M. Fuller (1998)

2. (Can explain recently observed He4 abundance in metal-poor galaxies)

A. Matsumoto et al., Astrophys. J. (2022)

- **How to generate such asymmetry?**

1. Decay of non-topological solitons predicted in MSSM
   →Consider the compatible parameter space to be consistent with sterile neutrino DM production

2. Observational implications on the stochastic GW background in this scenario

Introduction : dark matter

- Dark matter range

Consists of the ~ 20 % of the energy density of the universe
Has (almost) only the gravitational interactions

At present, a wide mass range is possible.

Depending on the spin statistics and the production mechanism,
some regions are limited.

In this talk, we focus on light sterile neutrinos as dark matter,
whose mass range is $\mathcal{O}(1) - \mathcal{O}(10)$ keV.

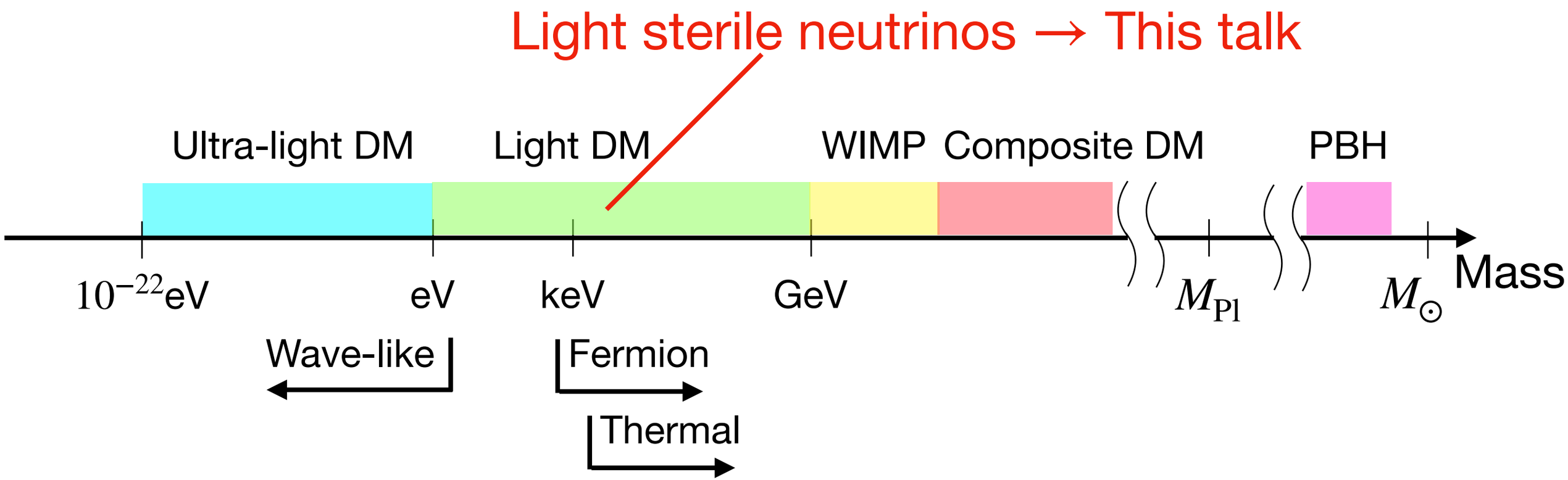

Introduction : Sterile neutrino dark matter

Sterile neutrino : $SU(3)_C \times SU(2)_W \times U(1)_Y$ gauge singlet fermion (ν_s)

$$\mathcal{L}_{\nu\mathrm{MSM}} \supset -m_s \overline{\nu_s^c} \nu_s - y_\alpha \overline{\ell_{L\alpha}} \epsilon \phi^* \nu_s + \mathrm{h.c.}$$

Motivated by origin of neutrino mass, etc…..

- The lightest sterile neutrino ((mass)$\sim \mathcal{O}(10)$keV) is a **dark matter** candidate.

For review, see A. Boyarsky et al., 1807.07938

- keV-scale sterile neutrino dark matter can be tested by

1. Effect on structure formation with $\sim \mathcal{O}(0.1)$ Mpc
   $\rightarrow$ can be probed by Lyman α forest method J. Baur et al., 1706.03118

2. **X-ray** observations
   via radiative decay $\nu_s \rightarrow \nu_\alpha + \gamma$ via mixing with SM neutrinos

A. Neronov et al., 1607.07328 (2016)

Dodelson-Widrow mechanism

Production of keV-scale sterile neutrinos
via **neutrino oscillation** involving active-sterile states :

Initial : Energy-eigenstate
$|\nu_1\rangle = \cos\theta\,|\nu_e\rangle - \sin\theta\,|\nu_s\rangle$

Interaction of $|\nu_e\rangle$ with thermal plasma →

Coherence breaking, $|\nu_s\rangle$ production

$|\nu_e\rangle, |\nu_s\rangle$: Flavor eigenstates $|\nu_1\rangle, |\nu_2\rangle$: mass eigenstates

Oscillation amplitude

$$\langle P(\nu_e \to \nu_s)\rangle = \frac{1}{2}\frac{\sin^2 2\theta}{\sin^2 2\theta + (\cos 2\theta + 2pV_e/m_s^2)^2}$$ (in thermal plasma)

$V_e \sim G_F^2 pT^4$: thermal self energy of **active** neutrinos

- Contour to explain all DM

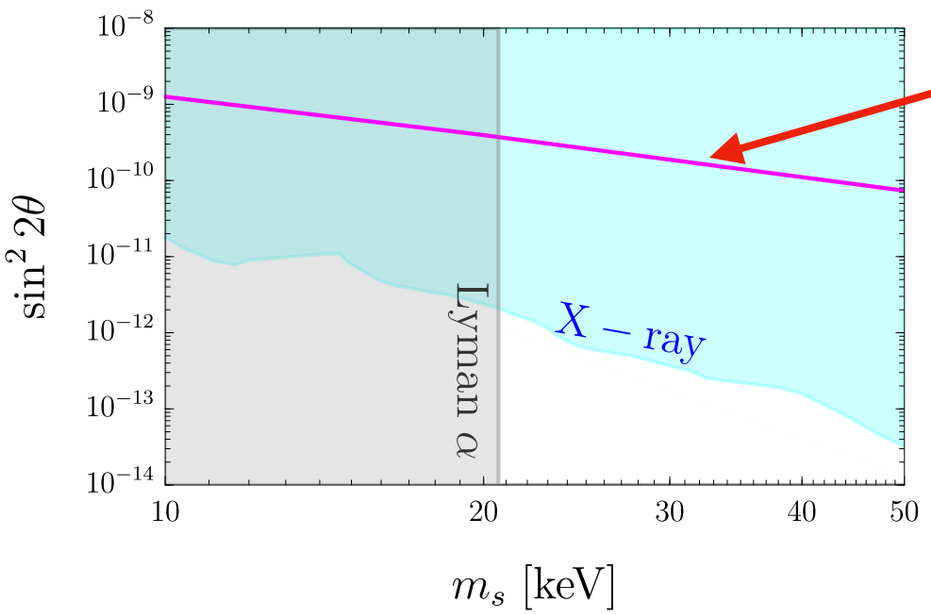

To explain All DM

→Severely constrained
by X-ray and Lyman α observations

Resonant production of sterile neutrinos

Consider lepton asymmetric thermal plasma.

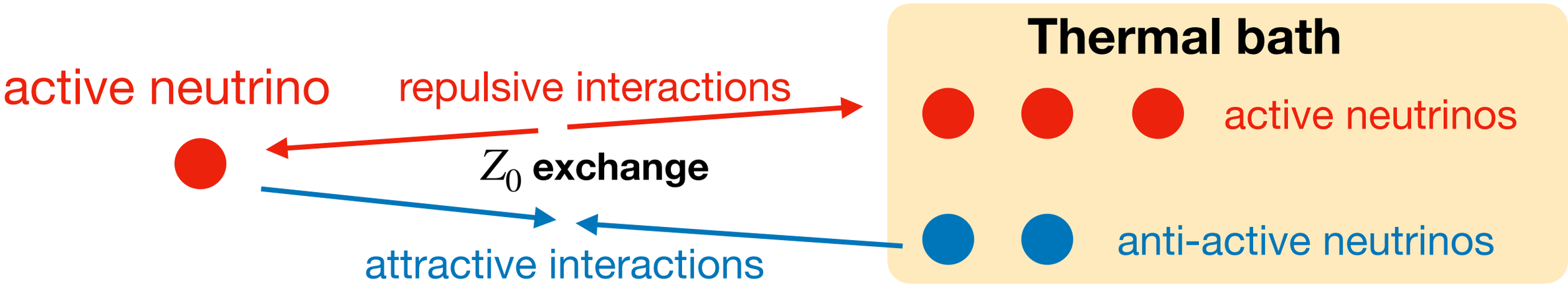

active neutrino self energy $\propto -(n_{\nu_a} - n_{\bar{\nu}_a})$ (lepton asymmetry)

Effective mixing angle :

$$\langle P(\nu_a \to \nu_s) \rangle = \frac{1}{2} \frac{\sin^2 2\theta_a}{\sin^2 2\theta_a + (\cos 2\theta + 2p(-8\sqrt{2} G_F s_{\rm tot} L_{\nu_a} + r_a G_F^2 p T^4)/m_s^2)^2}$$

$$= 0 : \textbf{Resonance}$$

$s_{\rm tot}$: total entropy density, $L_{\nu_a} \equiv (n_{\nu_a} - n_{\bar{\nu}_a})/s_{\rm tot}$: lepton asymmetry

Can explain all dark matter with smaller mixing angle.

Effective mixing angle with $p \simeq T$

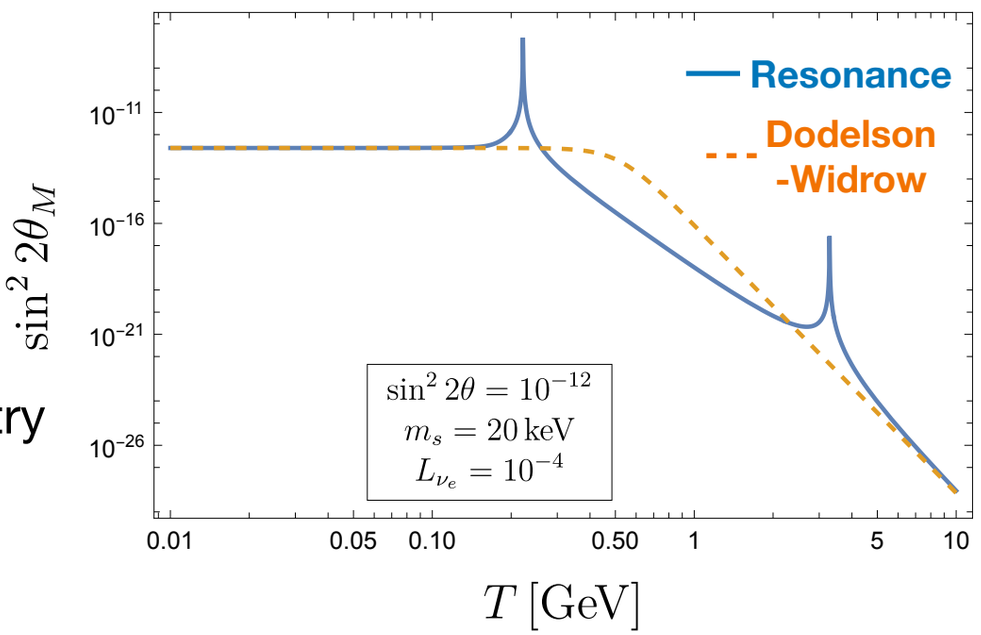

Large lepton asymmetry : recent observation

The resonance requires $(n_\nu - n_{\bar{\nu}})/s_{\rm tot} \gtrsim 10^{-5}$. A. Matsumoto et al., Astrophys. J. (2022)

Measurements of He4 in metal-poor galaxies determined primordial Helium abundance
$Y_P \equiv \rho_{\rm He4}/\rho_{\rm B} = 0.2370^{+0.0034}_{-0.0033}$
($\sim 1\sigma$ smaller than previous results)

Together with the Deuterium abundance observed in Cooke et al., (2018)
and baryon asymmetry determined by Planck 2018, they determined
$N_{\rm eff}$ and $L^{\rm init}_{\nu_e} \equiv (n_{\nu_e} - n_{\bar{\nu}_e})/s_{\rm tot}$

$$\rightarrow L^{\rm init}_{\nu_e} = 1.8^{+1.1}_{-0.7} \times 10^{-3}$$
$$N_{\rm eff} = 3.11^{+0.34}_{-0.31}$$

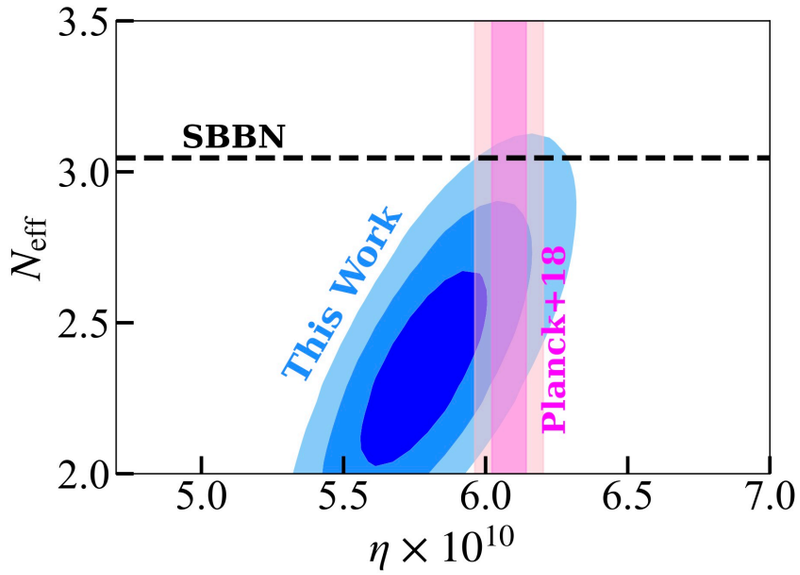

Figure : A. Matsumoto et al., Astrophys. J. (2022)

Today's talk

1. Numerical analysis of Resonant production scenario of light sterile neutrinos

2. Generation of large lepton asymmetry

3. Observational implications

1. Numerical analysis of Resonant production scenario of light sterile neutrinos

Details in formalism on sterile neutrino production

- Master equation

A. D. Dolgov (2002), T. Asaka, M. Shaposhnikov (2005)

$$i(\partial_t - Hp\partial_p)\rho = \underbrace{[\mathcal{H}, \rho]}_{\text{neutrino oscillation with matter effect}} - \underbrace{i\{\Gamma, \rho - \rho_{\rm eq}\}}_{\text{active neutrino scattering with thermal plasma}}$$

$\rho(t,p) \equiv |\nu_a\rangle\langle\nu_a| + |\nu_s\rangle\langle\nu_s|$: density operator

$$\mathcal{H} = \begin{pmatrix} -\frac{m_s^2}{4p}\cos 2\theta & \frac{m_s^2}{4p}\sin 2\theta \\ \frac{m_s^2}{4p}\sin 2\theta & \frac{m_s^2}{4p}\cos 2\theta \end{pmatrix} + \begin{pmatrix} V_a & 0 \\ 0 & 0 \end{pmatrix},$$

: effective Hamiltonian taking matter effect into account

$$V_a \equiv \sqrt{2}G_{\rm F}\left(2(n_{\nu_a} - n_{\bar{\nu}_a}) + \sum_{b\neq a}(n_{\nu_b} - n_{\bar{\nu}_b})\right) - B_a p T^4$$

Causes resonance

: finite density/temperature potential of active neutrino

$B_e \simeq 10.88 \times 10^{-9}\text{GeV}^{-4}$

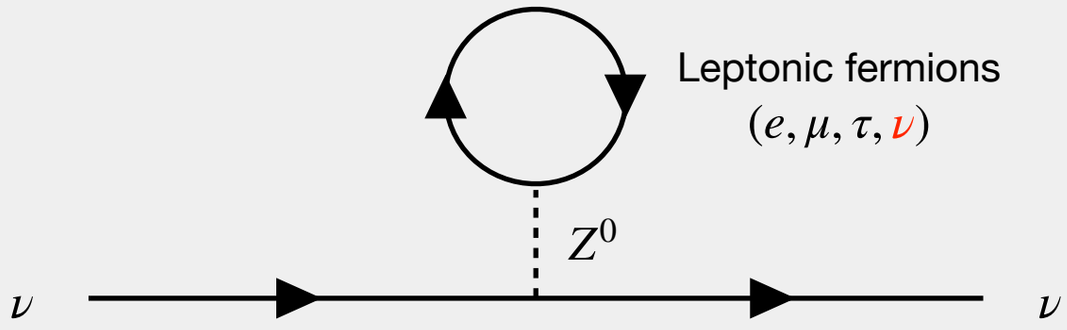

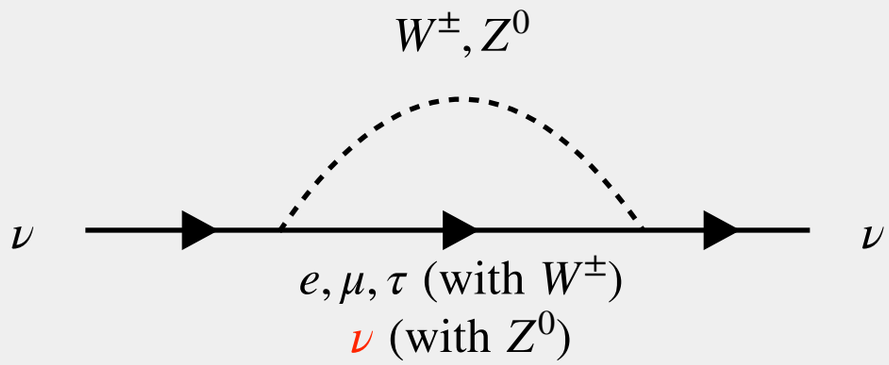

$$\Gamma = \frac{1}{2}\begin{pmatrix} \Gamma_{\nu_a} & 0 \\ 0 & 0 \end{pmatrix}$$

: scattering matrix

($\Gamma_{\nu_a}(p,T) \sim G_{\rm F}^2 p T^4$: neutrino interaction rate with thermal plasma)

Details in formalism on sterile neutrino production

- Master equation　　A. D. Dolgov (2002)　KK, K. Murai, M. Kawasaki, 2402.11902

$$
\begin{aligned}
i(\partial_t - Hp\partial_p)\rho_{aa} &= \frac{m_s^2}{4p}\sin 2\theta(\rho_{as}^* - \rho_{as}) - i\Gamma_{\nu_a}(\rho_{aa} - f_{\rm eq}) \ , \\
i(\partial_t - Hp\partial_p)\rho_{ss} &= \frac{m_s^2}{4p}\sin 2\theta(\rho_{as} - \rho_{as}^*) \ , \\
i(\partial_t - Hp\partial_p)\rho_{as} &= \frac{m_s^2}{4p}\sin 2\theta(\rho_{ss} - \rho_{aa}) + \left(V_a - \frac{m_s^2}{2p}\cos 2\theta - i\frac{\Gamma_{\nu_a}}{2}\right)\rho_{as}
\end{aligned}
$$

- Stationary point approximation : $i(\partial_t - Hp\partial_p)\rho_{as} \simeq 0$

- Master equation of sterile neutrino distribution function :

$$
(\partial_t - Hp\partial_p) f_{\nu_s}(p,T) = \Gamma_{\nu_a}(p,T)\left[\underbrace{\theta_M^2(p,T) f_{\nu_a}(p,T)}_{\nu_a \to \nu_s} + \underbrace{\bar{\theta}_M^2(p,T) f_{\bar{\nu}_a}(p,T)}_{\bar{\nu}_a \to \nu_s}\right]
$$

where　$f_{\nu_a} \equiv \rho_{aa}, \ f_{\nu_s} \equiv \rho_{ss}$

$$
\theta_M^2(p,T) \equiv \theta^2 \left[\left(1 - \frac{2p}{m_s^2}V_a(p,T)\right)^2 + \frac{p^2\Gamma_{\nu_a}^2(p,T)}{m_s^4}\right]^{-1} ,
$$

$$
\bar{\theta}_M^2(p,T) \equiv \theta^2 \left[\left(1 - \frac{2p}{m_s^2}V_{\bar{a}}(p,T)\right)^2 + \frac{p^2\Gamma_{\nu_a}^2(p,T)}{m_s^4}\right]^{-1} .
$$

where　$V_{\bar{a}} = \sqrt{2}G_{\rm F}\left(-2(n_{\nu_a} - n_{\bar{\nu}_a}) + \sum_{b\neq a}(-n_{\nu_b} + n_{\bar{\nu}_b})\right) - B_a p T^4$

Details in formalism on sterile neutrino production

- **Numerical setup**

KK, K. Murai, M. Kawasaki, 2402.11902
See also J. Ghiglieri, M. Laine, 1506.06752

- The epoch at sterile neutrino DM production coincides with QCD phase transition
  → should carefully take time evolution of g_* and total entropy conservation into account

  - Number of (active + sterile) is conserved :

$$\frac{n_{\nu_a} + n_{\bar{\nu}_a} + n_{\nu_s}}{s_{\rm tot}} = \text{const.}$$

$$\epsilon \equiv \left(\frac{g_{*,s}(T_i)}{g_{*,s}(T)}\right)^{1/3} \frac{p}{T}$$

: dimensionless mode

$$\epsilon_{\rm phys} \equiv p/T$$

: dimensionless physical mode

  - Time evolution of lepton asymmetry :

$$\frac{\mathrm{d}}{\mathrm{d}t} L_{\nu_e}(T) = \frac{45}{4\pi^4 g_{*,s}(T_i)} \int \mathrm{d}\epsilon\, \epsilon^2 \Gamma_{\nu_e}(p,T) \left[\theta_M^2(\epsilon,T) f_{\nu_e}(\epsilon,T) - \bar{\theta}_M^2(\epsilon,T) f_{\bar{\nu}_e}(\epsilon,T)\right]$$

$$\theta_M^2(\epsilon,T) \equiv \theta^2 \left[\left(1 - \frac{2p}{m_s^2} V_a(\epsilon,T)\right)^2 + \frac{p^2 \Gamma_{\nu_a}^2(\epsilon,T)}{m_s^4}\right]^{-1},$$

$$\bar{\theta}_M^2(\epsilon,T) \equiv \theta^2 \left[\left(1 - \frac{2p}{m_s^2} V_{\bar{a}}(\epsilon,T)\right)^2 + \frac{p^2 \Gamma_{\nu_a}^2(\epsilon,T)}{m_s^4}\right]^{-1}$$

$= 0 \leftrightarrow$ Resonance

Observation of numerical behavior : non- resonant case

- The case with $L_{\nu_e} = 0$ (DW mechanism)
  → Non-resonant production

G. B. Gelmini et al., 1909.13328v2

- Assumption : only mixing between $\nu_s \leftrightarrow \nu_e$

Production rate with $\epsilon = 1$:

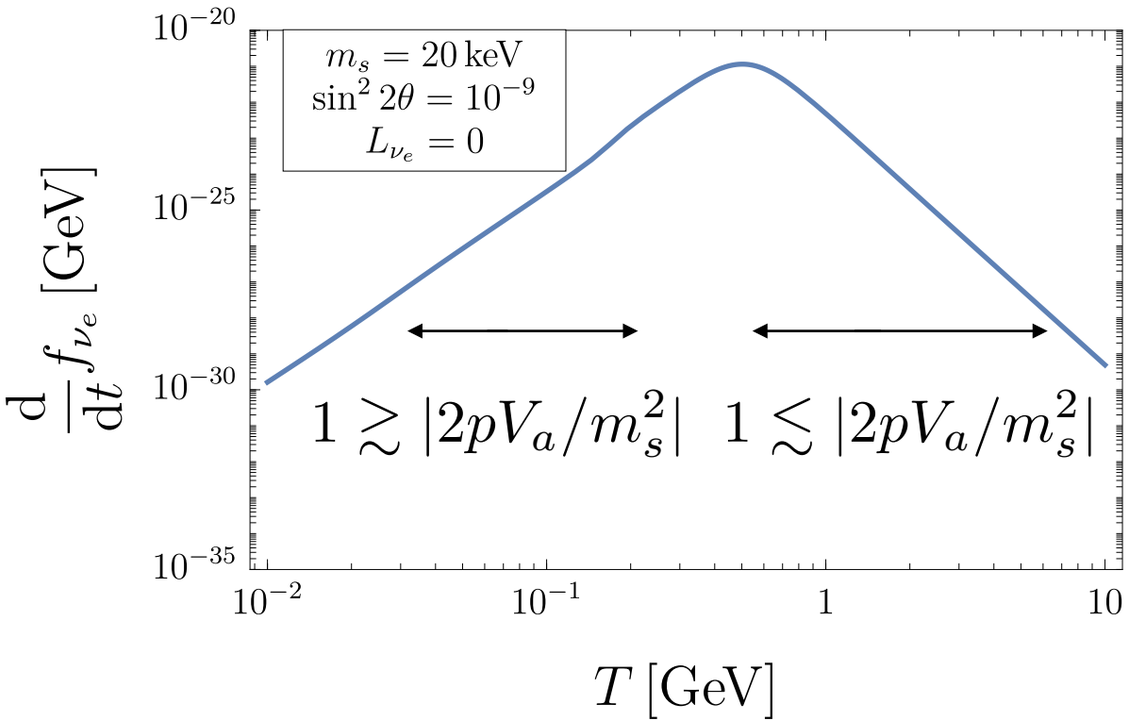

- Temperature at production peak :

$$\leftrightarrow T \sim T_{\mathrm{peak}} \equiv 0.31\,\mathrm{GeV} \left(\frac{m_s}{10\,\mathrm{keV}}\right)^{1/3} \epsilon_{\mathrm{phys}}^{-1/3}$$

- Final spectrum is proportional to

$$\theta^2 f_{\nu_e}(T = T_{\mathrm{peak}})$$

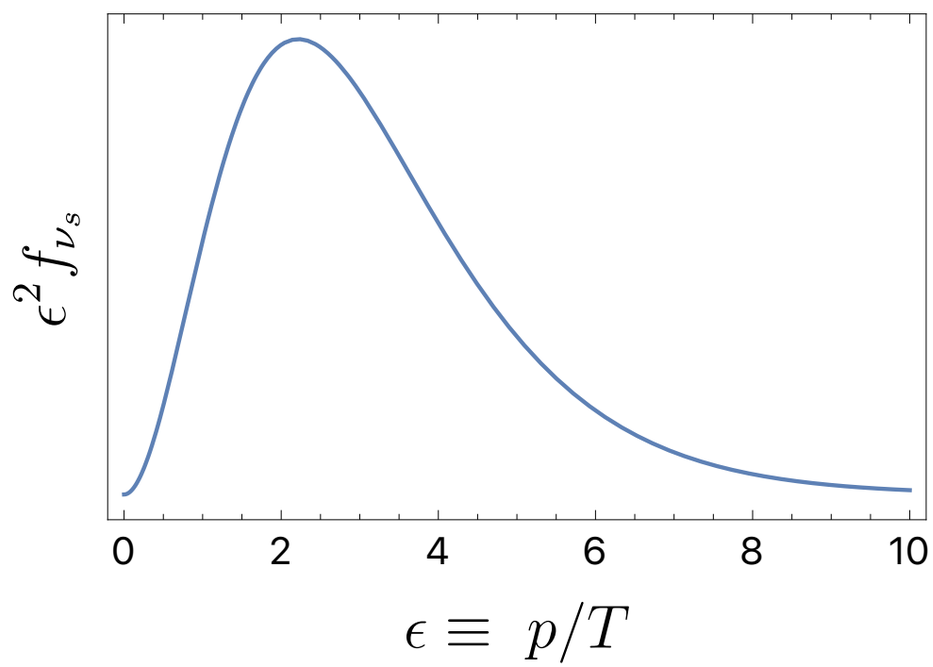

Observation of numerical behavior : resonant case

KK, K. Murai, M. Kawasaki, 2402.11902

Production rate with $\epsilon = 1$:

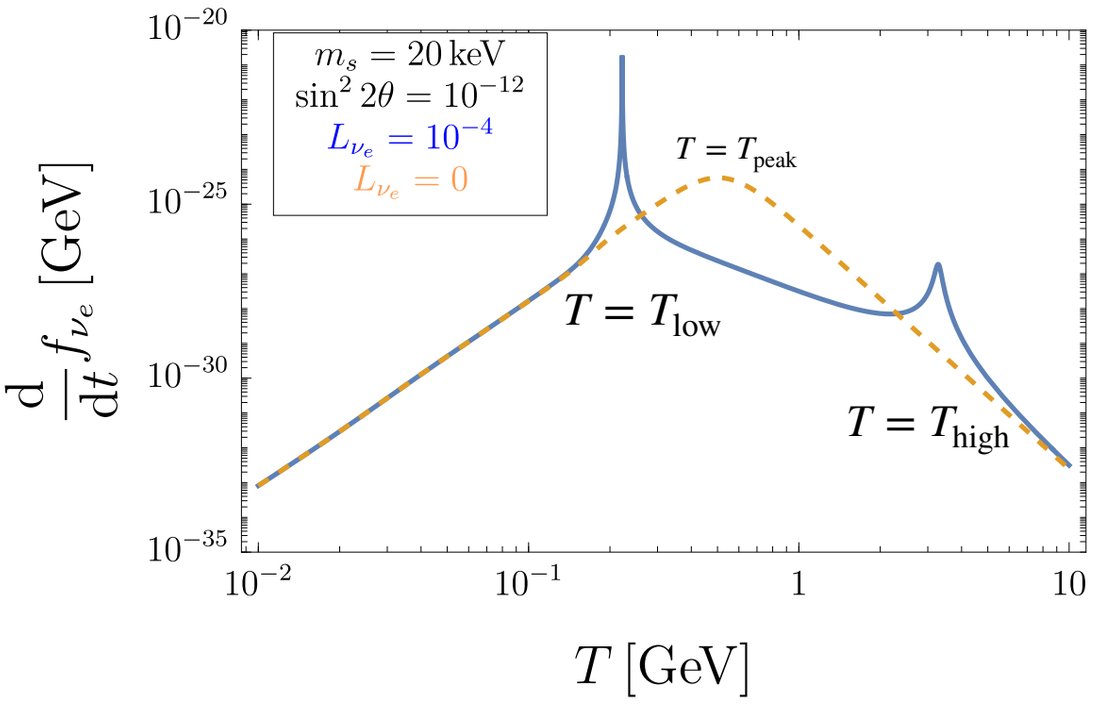

Resonance condition :

$$1 - \frac{2\epsilon_{\mathrm{phys}}(T)T}{m_s^2} V_e(\epsilon, T) = 0$$

$$\Leftrightarrow\ 1 - \frac{8\sqrt{2}\pi^2 g_*(T) G_{\mathrm{F}}}{45} \frac{\epsilon_{\mathrm{phys}}(T) L_{\nu_e} T^4}{m_s^2} + 2B_e \frac{\epsilon_{\mathrm{phys}}^2(T) T^6}{m_s^2} = 0$$

$$\leftrightarrow T = T_{\mathrm{low}}, T_{\mathrm{high}} \quad \left(T_{\mathrm{low}} \propto \frac{m_s^{1/2}}{L_{\nu_e}^{1/4} \epsilon^{1/4}},\ \ T_{\mathrm{high}} \propto \frac{L_{\nu_e}^{1/2}}{\epsilon^{1/2}} \right)$$

$$\epsilon_{\mathrm{phys}} \equiv p/T$$

$$\epsilon \equiv \left(\frac{g_{*,s}(T_i)}{g_{*,s}(T)} \right)^{1/3} \frac{p}{T}$$

- L_{ν_e} is consumed <u>from low ϵ mode to high ϵ mode</u>
- When L_{ν_e} is sufficiently consumed, the 2 resonance peaks disappear
  → after that, non-resonant production→ Leads to “cooler” distribution
- The epoch at sterile neutrino DM production coincides with QCD phase transition
  → should carefully take time evolution of g_* and total entropy conservation into account

Observation of numerical behavior : resonant case

Here, we perform a comprehensive parameter scan of the resonantly-produced sterile neutrinos for all DM.

Previous comprehensive search assumed that the lepton asymmetry is always equillibriated among the active neutrino three flavors

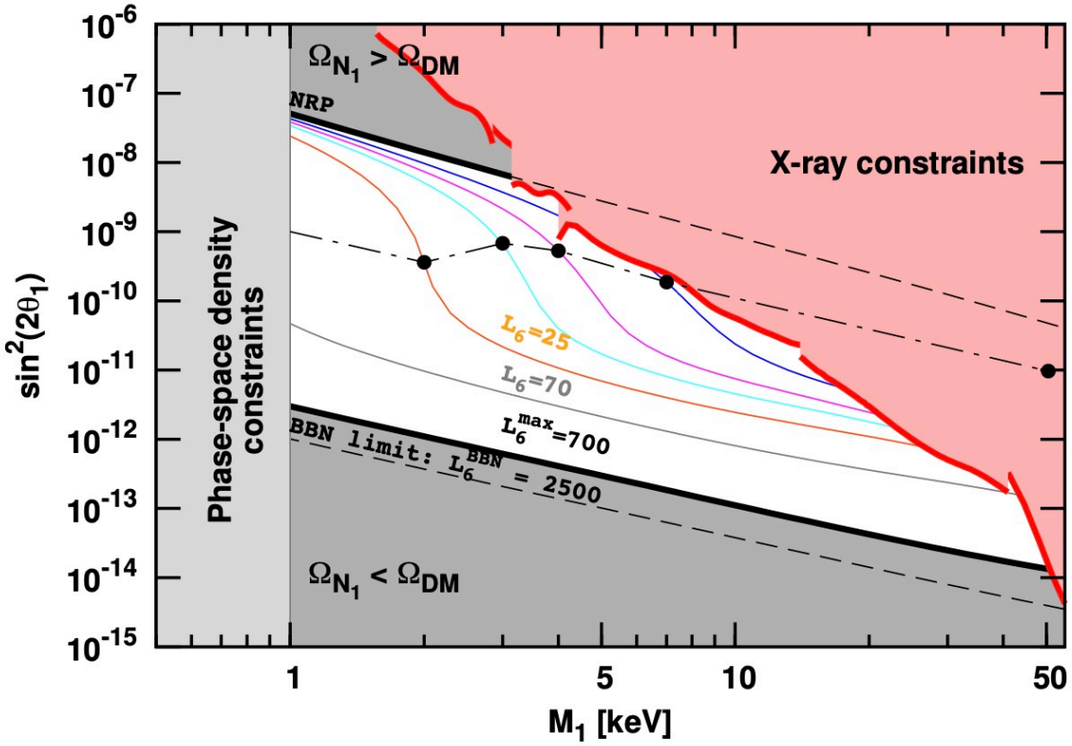

Figure :
M. Laine and M. Shaposhnikov,
JCAP06 (2008)

↔ Since the flavor oscillations takes place well after the resonant production ($T \lesssim \mathcal{O}(10)$MeV), we should switch-off the flavor oscillations

M. Ghiglieri and M. Shaposhnikov,
JHEP11 (2015)

Dependence on discretization method of momentum bins

- The decrease of L_{ν_e} due to production of a resonant mode backreacts to the production rate of other nearby modes
  → **strong mode coupling**
- The resonance peaks are **very sharp**
  → Very fine resolution is required for mode discretization!!

Ex.) If we discritize the modes linearly…..

$$\epsilon \equiv \left(\frac{g_{*,s}(T_i)}{g_{*,s}(T)}\right)^{1/3} \frac{p}{T}$$

$$\epsilon = \epsilon_{\rm max} \cdot i/N_{\rm bin},\ \epsilon_{\rm max} = 20$$

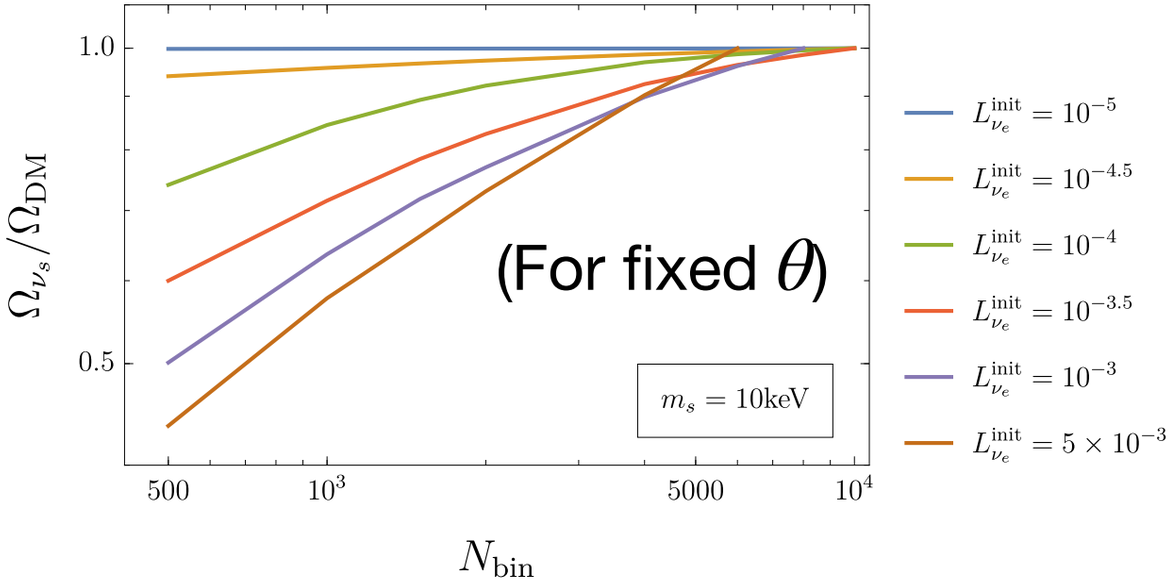

→ Strong dependence of the final abundance on bin number $N_{\rm bin}$ (For $L_{\nu_e}^{\rm init} \gtrsim 10^{-4}$)

↔ Only $N_{\rm bin} = 200$ is adopted by J. Ghiglieri, M. Laine, 1506.06752

→ **Our strategy** : Time-dependent discretization s.t. the modes around the resonance are most finely discritized

Dependence on discretization method of momentum bins

Time-dependent transformation of the momentum bins :

$$u(\epsilon) \equiv \frac{\epsilon - \epsilon_{\min}}{\epsilon_{\max} - \epsilon_{\min}} \qquad u = u_{\rm res}(T) + \alpha\left(v - v_{\rm res}(T)\right) + \beta(T)\left(v - v_{\rm res}(T)\right)^3$$

Where $\epsilon_{\rm res}$: Resonant mode

Original basic variables of QKE : $(\epsilon, T) \rightarrow$ New variable : (v, T)

Discritization of $0 < v < 1$ linearly with $N_{\rm bin} \sim 500$
automatically ensures the fine resolution around the resonant mode

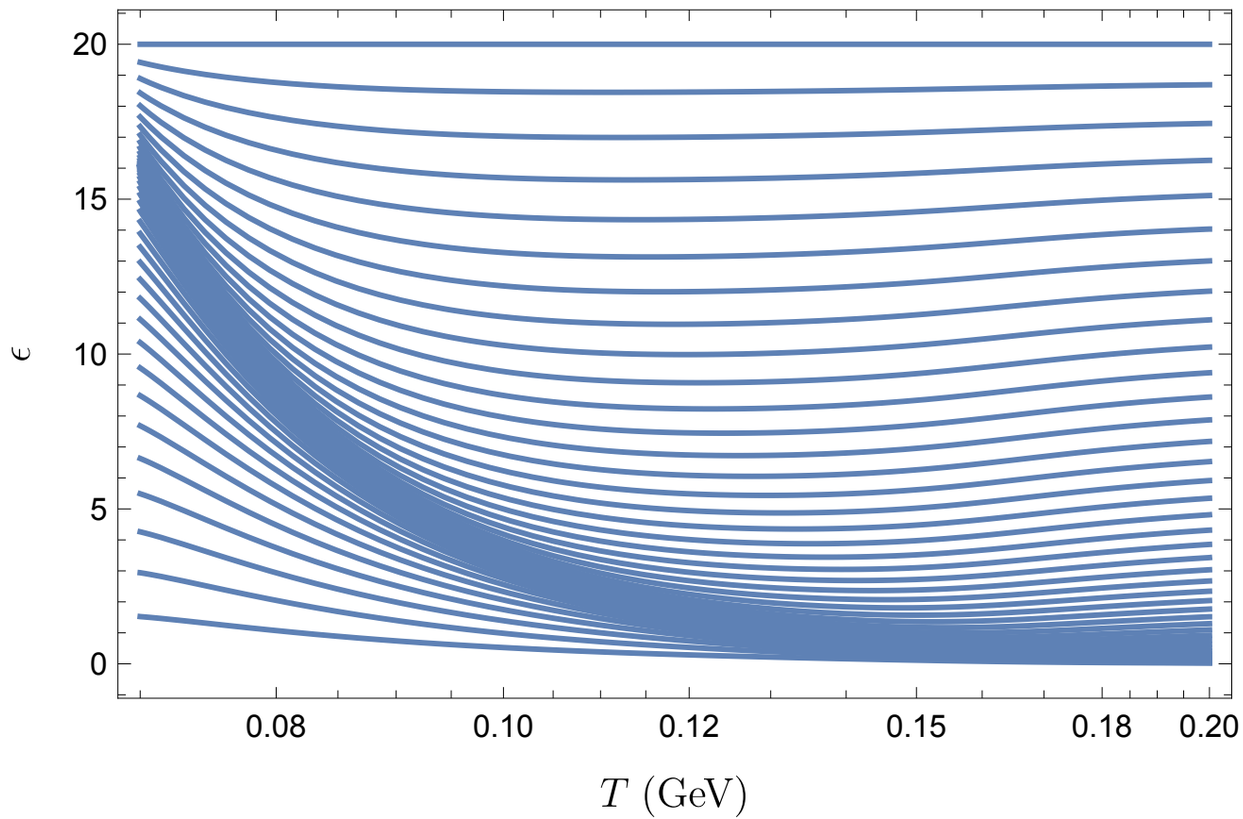

Blue lines : $v = \text{const.}$

Dependence on discretization method of momentum bins

Time-dependent transformation of the momentum bins :

$$u(\epsilon) \equiv \frac{\epsilon - \epsilon_{\min}}{\epsilon_{\max} - \epsilon_{\min}} \qquad u = u_{\rm res}(T) + \alpha\left(v - v_{\rm res}(T)\right) + \beta(T)\left(v - v_{\rm res}(T)\right)^3$$

Where $\epsilon_{\rm res}$: Resonant mode

Original basic variables of QKE : $(\epsilon, T) \rightarrow$ New variable : (v, T)

Discritization of $0 < v < 1$ linearly with $N_{\rm bin} \sim 500$
automatically ensures the fine resolution around the resonant mode

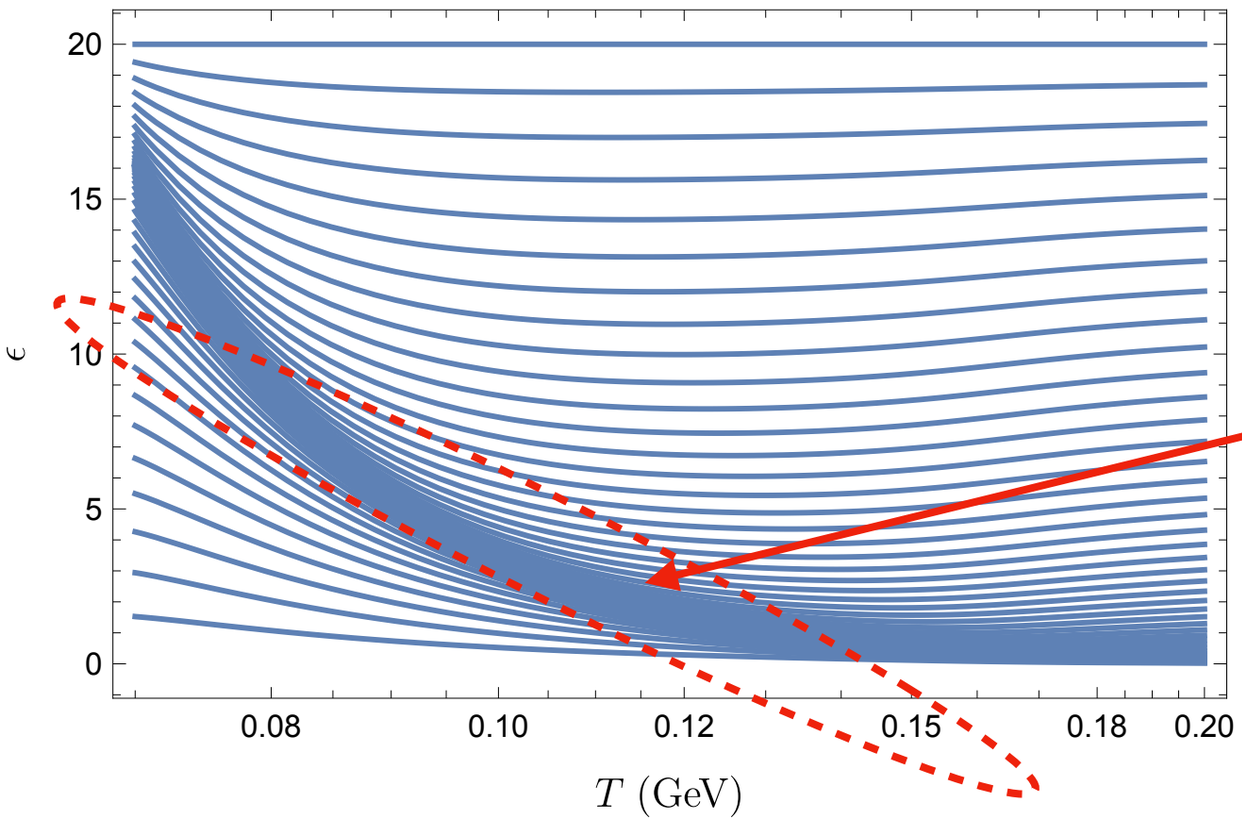

Blue lines : $v = \text{const.}$

Regions under resonance

Numerical Result 1.
Final spectrum of sterile neutrino DM

Numerical result (θ is fixed to explain all DM)

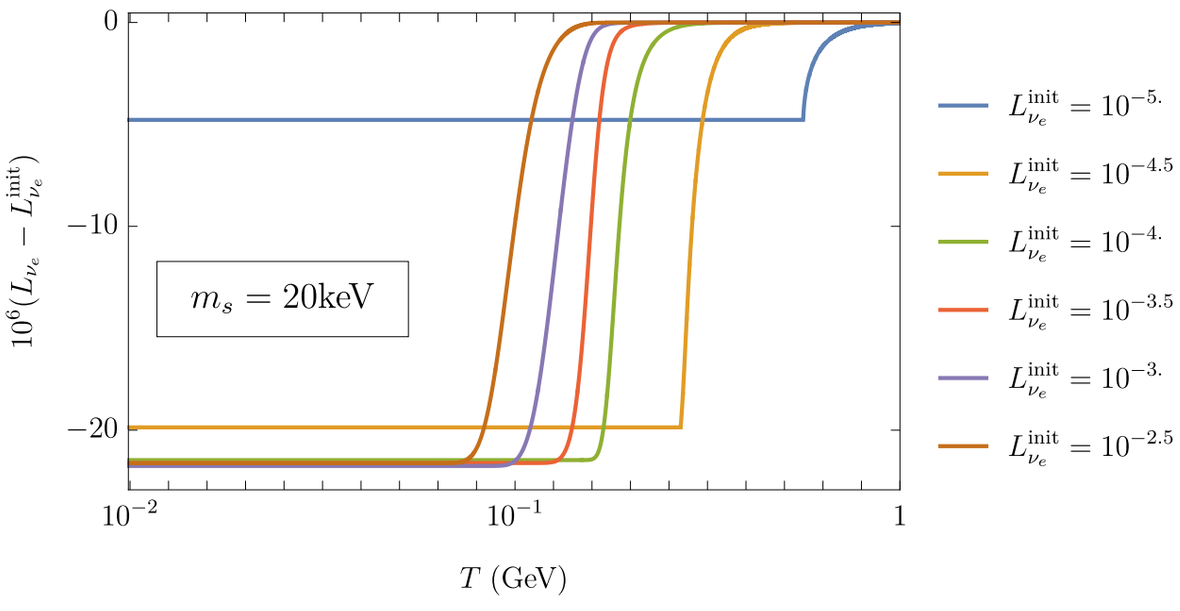

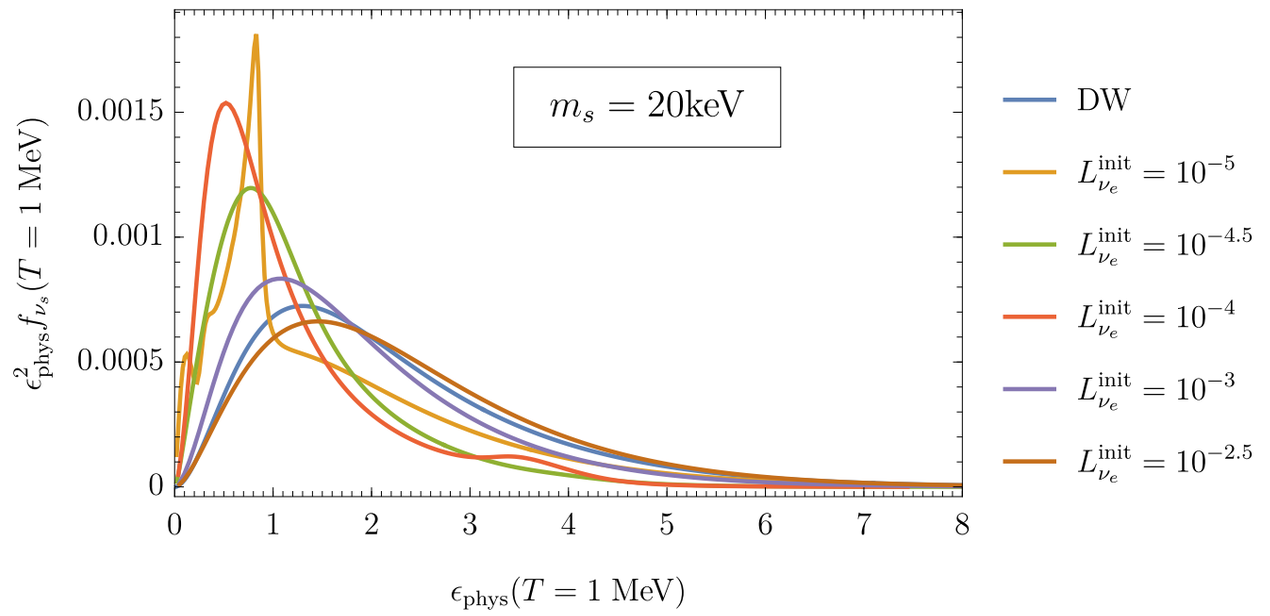

Approximate analytic result :

$$f_{\nu_s} \simeq 0.96 \frac{g_*(T_i)^{2/3}}{g_*(T_{\rm low})^{13/6}} \frac{M_{\rm Pl} m_s^4 \theta^2}{G_{\rm F} \epsilon^2 T_{\rm low}^7} \frac{f_{\nu_e}(\epsilon, T_{\rm low})}{L_{\nu_e}(T_{\rm low})} \propto \frac{m_s^{1/2} L_{\nu_e}^{3/4} \theta^2}{\epsilon^{1/4}} f_{\nu_e}$$

- Final spectrum is proportional to $L_{\nu_e}^{3/4}$
- If the time evolution of L_{ν_e} is significant, the final spectrum gets further cooler than thermal distribution
- If the time evolution of L_{ν_e} is negligible, the final spectrum is proportional to $\epsilon^{-1/4} \times$ (thermal distribution)

Numerical Result 3. Observational constraints

KK, K. Murai, M. Kawasaki, 2402.11902

m_s - θ contour to explain all DM

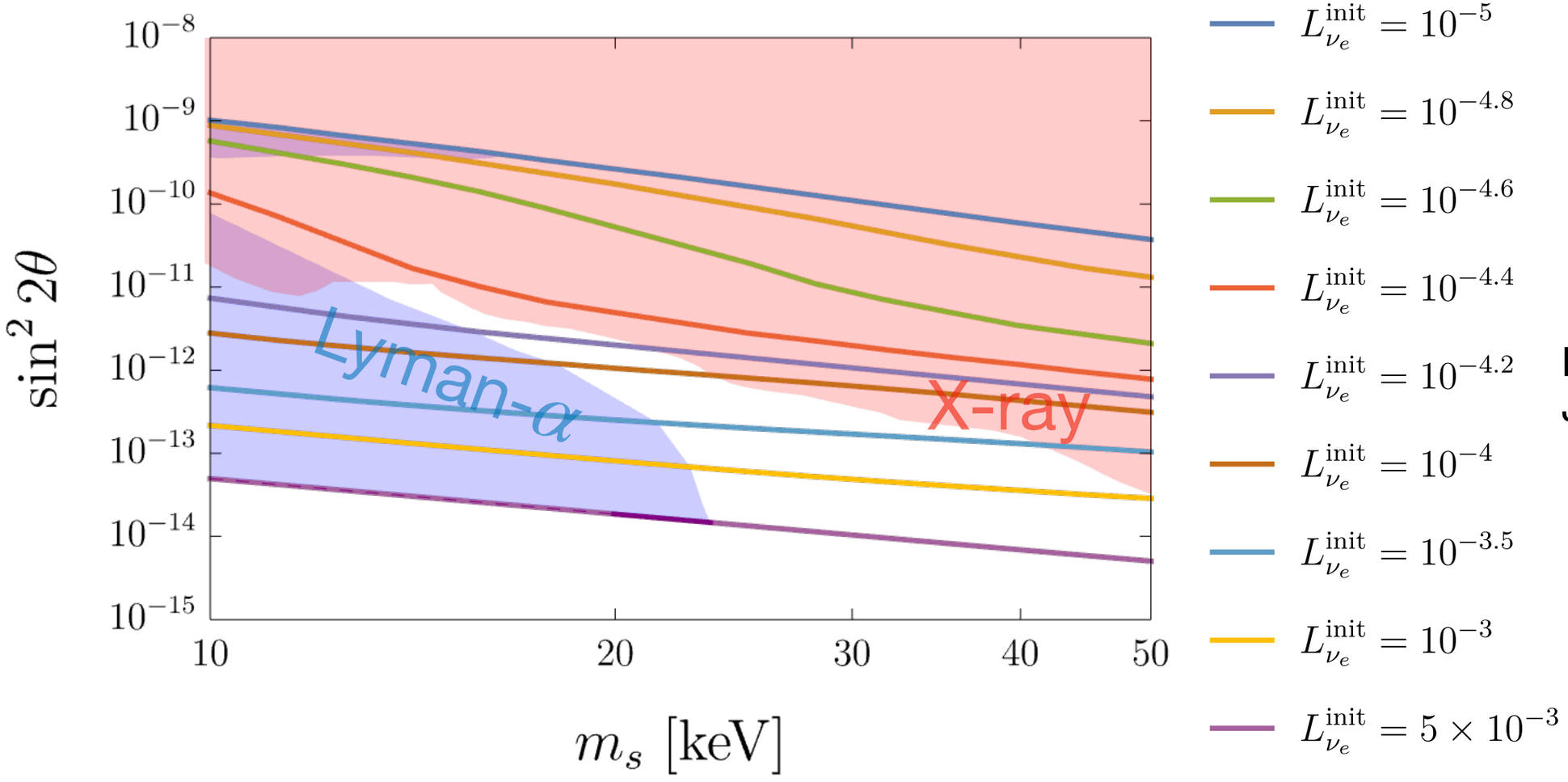

Lyman-α :
J. Baur et al., 1706.03118

- Small $L_{\nu_e}^{\rm init}(\lesssim 10^{-4.5})$ → the final spectrum is cool→ the Lyman α constraint is weak
- Large $L_{\nu_e}^{\rm init}(\gtrsim 10^{-4.5})$ → the final spectrum is warm and the production temperature is low → the Lyman α constraint is strong
- This scenario requires **large lepton asymmetry** with $L_{\nu_e}^{\rm init} \gtrsim \mathcal{O}(10^{-4})$

Numerical analysis of resonant production scenario :Discussions

KK, K. Murai, M. Kawasaki, 2402.11902

- The “stationary point” approximation

  We approximate off-diagonal component of the density matrix by stationary-solutions:

$$\rho_{as} \simeq \rho_{as,\mathrm{stat}} \equiv -\frac{\sin 2\theta}{2\cos 2\theta - \frac{2p}{m_{\nu_s}^2}(2V_a - i\Gamma_{\nu_a})}\rho_{aa}.$$

  For our treatment to be valid :

$$\delta t_{\mathrm{res}} \equiv \left.\frac{\mathrm{d}t}{\mathrm{d}T}\right|_{T_{\mathrm{res}}} \times \frac{\Gamma_{\nu_a}(T_{\mathrm{res}})T_{\mathrm{res}}}{3V_a(\epsilon_{\mathrm{phys}}, T_{\mathrm{res}})} \gg \Gamma_{\nu_a}^{-1} \Leftrightarrow D_{\mathrm{stat}} \equiv \delta t_{\mathrm{res}} \cdot \Gamma_{\nu_a} \gg 1$$

δt_{res} : timescale of the resonance of a given mode

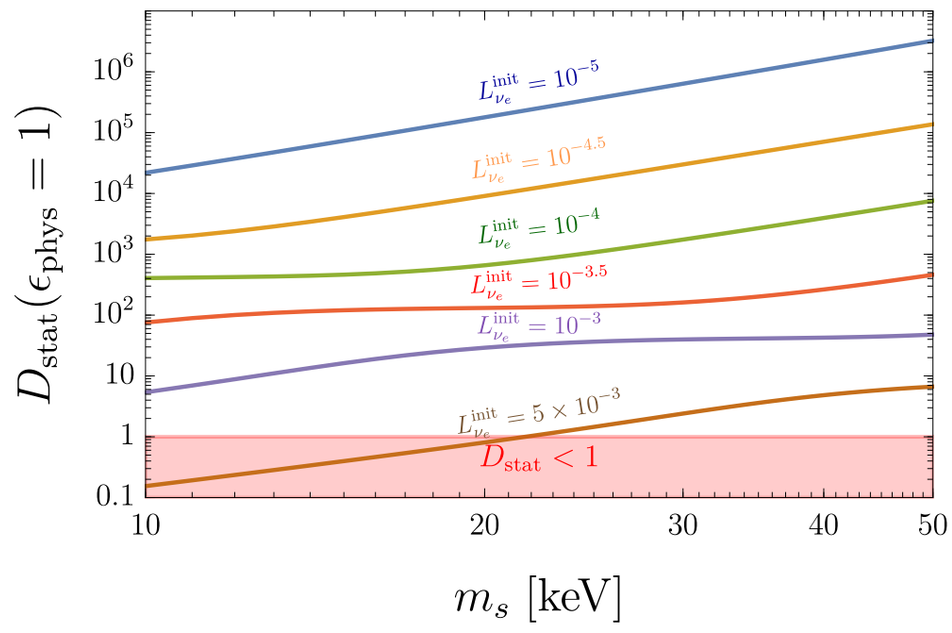

2. Generation of large lepton asymmetry

Generation of large lepton asymmetry

If the lepton asymmetry is generated before the electroweak phase transition $T_{\rm ew} \sim 100$ GeV, the baryon asymmetry with the same order is produced via sphaleron process.

To explain large hierarchy between lepton/baryon asymmetry,
lepton asymmetry must be produced after the freeze-out of the sphaleron process.

- CP violation in decay of the other heavy sterile neutrino
  : $L_{\nu_e} \lesssim 7 \times 10^{-4}$ can be generated

  M. Shaposhnikov (2008)

- This talk : Affleck-Dine leptogenesis
  : Even larger asymmetry with $L_{\nu_e} \gtrsim \mathcal{O}(10^{-3})$, which is compatible with the resonance of ν_s production, can be generated.

Affleck-Dine (AD) leptogenesis

- Potential

I. Affleck, M. Dine (1985), M. Dine, L. Randoll, S. D. Thomas (1996)

$$V(\phi) \simeq m_{3/2}^2|\phi|^2 - cH^2|\phi|^2 + |\lambda|^2 \frac{|\phi|^{2(n-1)}}{M_{\rm Pl}^{2n-6}} + \lambda a_{\rm M} \frac{m_{3/2}\phi^n}{nM_{\rm Pl}^{n-3}} + {\rm h.c.}$$

ϕ : Leptonic flat direction in MSSM (=**AD field**) Ex.) $L_1 L_2 \bar{e}_2$

$m_{3/2}$: "gravitino" mass, H : Hubble parameter, $a_M = \mathcal{O}(1)$, $c(>0) = \mathcal{O}(1)$

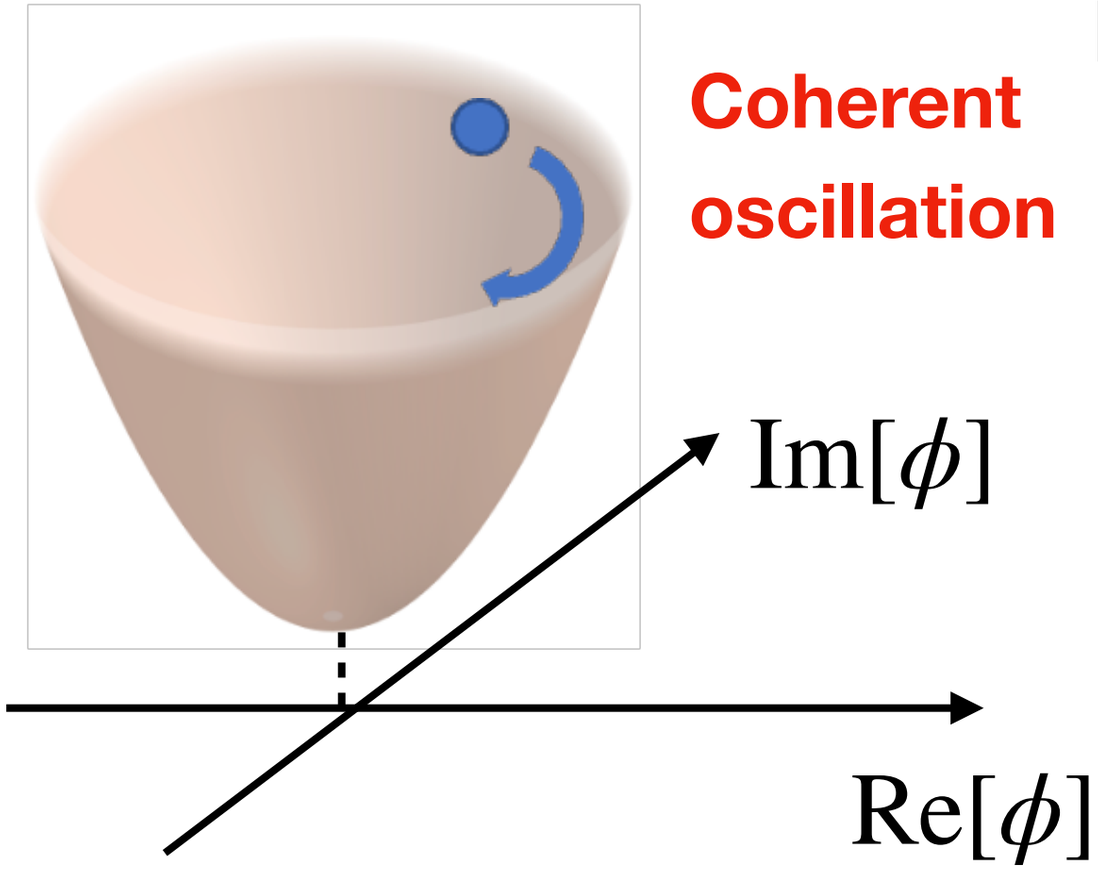

Coherent oscillation

Lepton number $\leftrightarrow$ global $U(1)$ sym.

Rotation of ϕ
↓
lepton number generation.

Resultant lepton number :

$$n_{\rm L} = i\left(\phi^*\dot{\phi} - \dot{\phi}^*\phi\right) \simeq \dot{\theta}|\phi|^2$$
$$\simeq \epsilon m_{3/2}\varphi_{\rm osc}^2$$

ϵ : efficiency parameter
determined by $\arg(a_M)$, λ, etc.

Q-balls

- Q-ball solution (General case)

  = Spherically symmetric (non-topological) solitons of ϕ, stabilized by $U(1)$ symmetry

Consider a complex scalar field ϕ with global $U(1)$ symmetry

$$\mathcal{L} = \partial_\mu \phi^* \partial^\mu \phi - V(|\phi|)$$

Global $U(1)$ charge :

$$Q = -i \int \mathrm{d}^3 x (\phi^* \dot{\phi} - \phi \dot{\phi}^*)$$

Total energy :

$$E = \partial_\mu \phi^* \partial^\mu \phi + V(|\phi|)$$

Q-ball : Spherically symmetric field configuration
that minimizes E with fixed Q

→ Minimize $\quad E_\omega \equiv E + \omega \left[Q + i \int \mathrm{d}^3 x (\phi^* \dot{\phi} - \phi \dot{\phi}^*) \right]$

Lagrange multiplier

Q-balls

Q-ball : Configuration that minimizes E with fixed Q

$$E_\omega \equiv E + \omega\left[Q + i\int \mathrm{d}^3x(\phi^*\dot{\phi} - \phi\dot{\phi}^*)\right]$$

$$= \int \mathrm{d}^3x|\partial_t\phi - i\omega\phi|^2 + \int \mathrm{d}^3x\left[|\nabla\phi|^2 + V_\omega(\phi)\right] + \omega Q$$

$\partial_t\phi - i\omega\phi$ → 0

$|\nabla\phi|^2 + V_\omega(\phi)$ → Minimize

$$\rightarrow \quad \phi = e^{i\omega t}\varphi(r) \qquad \varphi : \text{spherical symmetric function}$$

$$\frac{\mathrm{d}^2\varphi}{\mathrm{d}r^2} + \frac{2}{r}\frac{\mathrm{d}\varphi}{\mathrm{d}r} + \left[\omega^2\varphi(r) - \frac{\partial V(\varphi)}{\partial\varphi}\right] = 0$$

Condition that Q-ball solution exists with boundary condition :

$$\varphi'(r=0) = 0, \varphi(r\to\infty) = 0$$

$$\min\left[\frac{2V(\varphi)}{\varphi^2}\right]_{\varphi\neq 0} < \omega < V''(\varphi = 0)$$

Q-ball solution exists when the potential is flatter than the quadratic one.

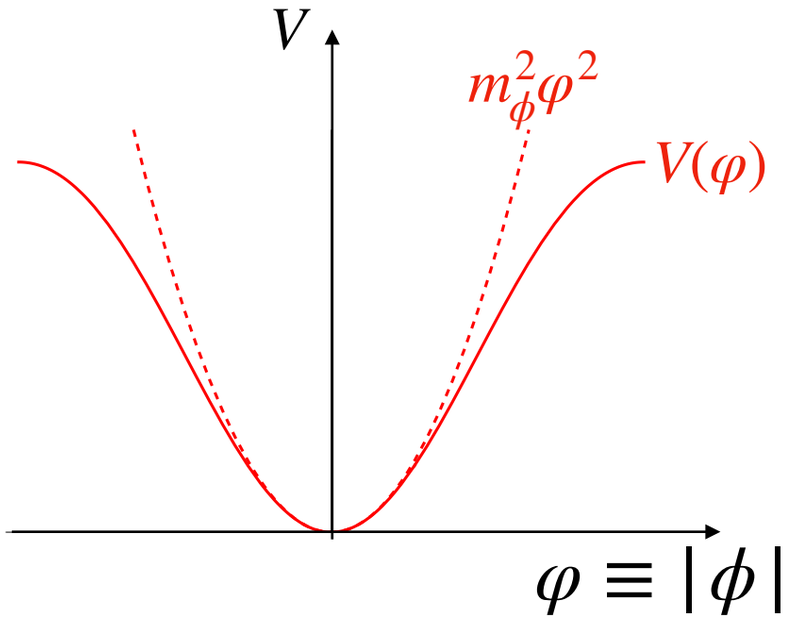

Formation of “Q-ball”s

Our setup

SUSY breaking potential : $V = V_{\rm gauge} + V_{\rm gravity}$

where $V_{\rm gauge} = M_{\rm F}^4 \left(\ln \frac{|\phi|^2}{M_S^2} \right)^2$,

$V_{\rm gravity} = m_{3/2}^2 \left[1 + K \ln \left(\frac{|\phi|^2}{M_{\rm Pl}^2} \right) \right] |\phi|^2$

$M_{\rm F} \equiv \sqrt{\langle F \rangle}$: SUSY breaking scale

$m_{3/2}$: Gravitino mass

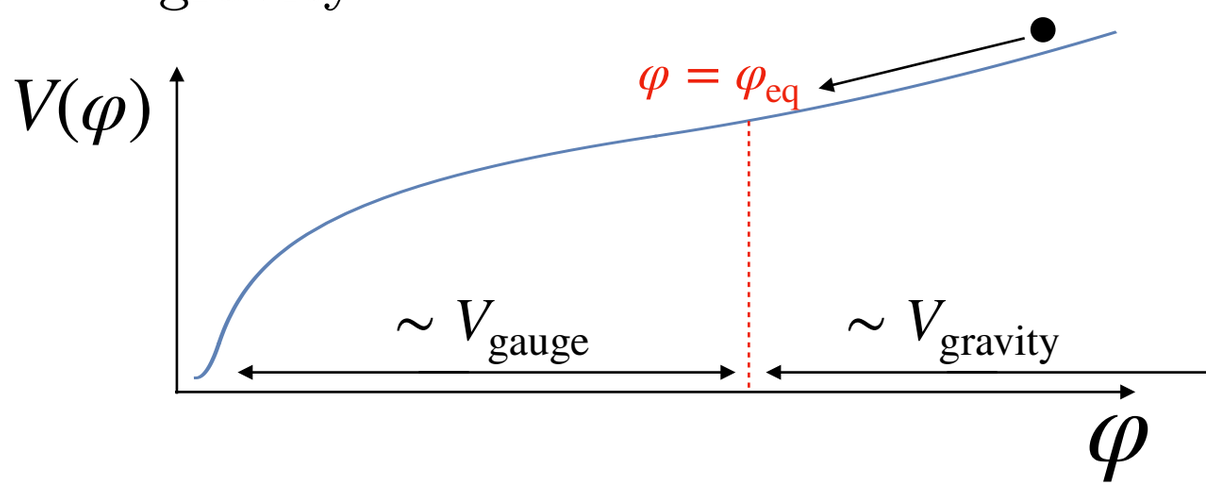

After coherent AD field oscillation, $V_{\rm gauge}$ begins to dominate and the AD field configuration has spatial instability and forms Q-balls.

Instability band of the field fluctuations: $R_Q \sim \frac{\varphi_{\rm eq}}{M_F^2}$

→ Properties of Q-balls : $\omega_Q = \sqrt{2}\pi\zeta M_F Q^{-1/4},\ Q = \beta \left(\frac{\varphi_{\rm eq}}{M_{\rm F}} \right)^4$

β, ζ : numerical constants

Inside the Q-ball, ϕ has a VEV of $\varphi \gg \mathcal{O}(100)$ GeV

→ Gauge boson has a huge mass due to the coupling with ϕ

→ Stable against sphaleron process, no baryon number is generated

Decay of Q-balls

Q-balls are classically stable, but decay into light fermions with masses $m_f < \omega$ through quantum effect.

If final states are fermions, decay process is bounded by Pauli-blocking effect of the final states

→upper bound of the decay rate is given by number of possible states of outgoing flow of the fermions

A. Cohen et al. (1986), M. Kawasaki, M. Yamada (2012)

In our case ($\phi =$ sleptons), Q-balls decay into SM neutrinos via $\phi\phi \to \nu\nu$ process (via Zino/Higgsino exchange)

Saturated decay takes place in realistic situations

→decay rate is given by

$$\Gamma_Q \simeq \frac{1}{Q}\frac{\omega_Q^3}{\pi}\left(\frac{N_l}{3}\right) R_Q^2$$

N_l : Number of neutrino species

Large lepton asymmetry from Q-ball decay

Once (decay rate) $\sim H$ is satisfied, they instantaneously decay and lepton asymmetric thermal plasma is generated.

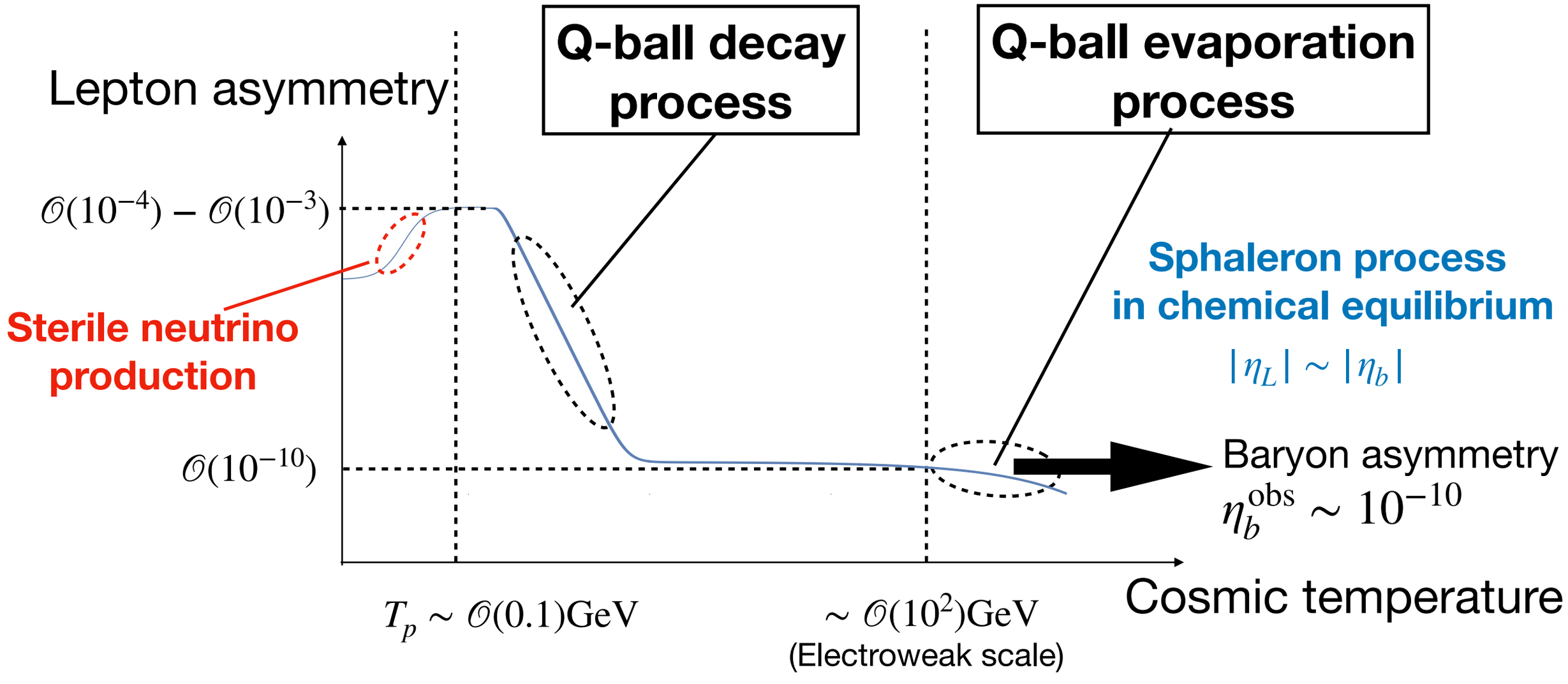

Large lepton asymmetry from Q-ball decay

KK, M. Kawasaki, K. Murai, 2402.11902

We estimate the allowed parameter space in Q-ball decay scenario which is compatible with Shi-Fuller mechanism.

(i.e. Q-ball decay producing lepton asymmetry $\gtrsim \mathcal{O}(10^{-4})$ occurs above the resonance temperature of sterile neutrino production $\sim \mathcal{O}(0.1)\mathrm{GeV}$)

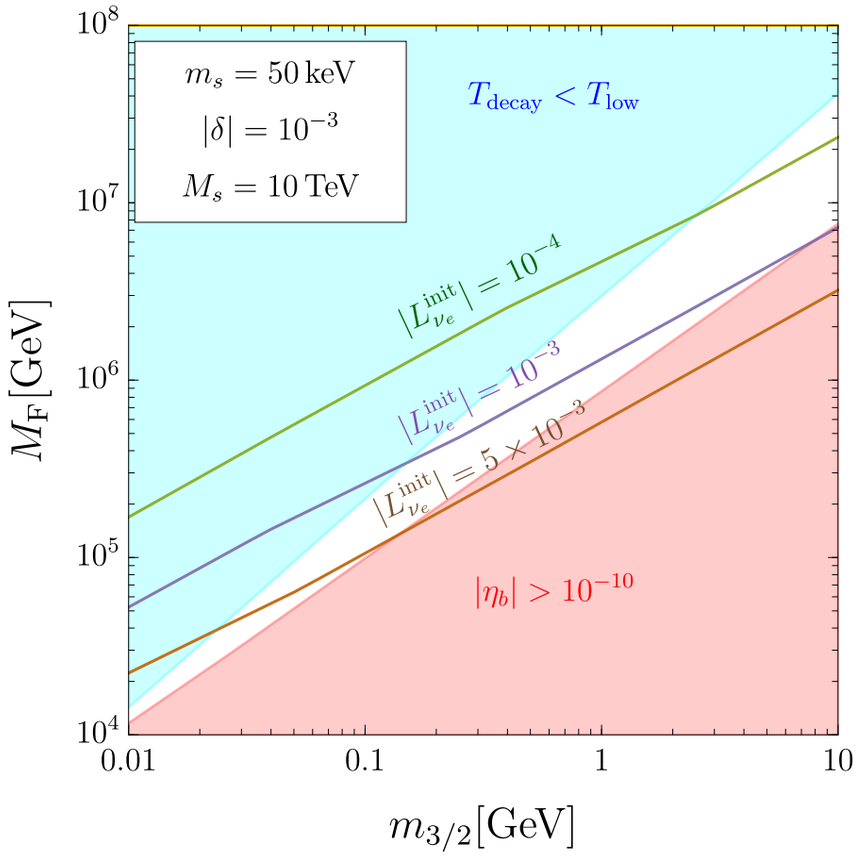

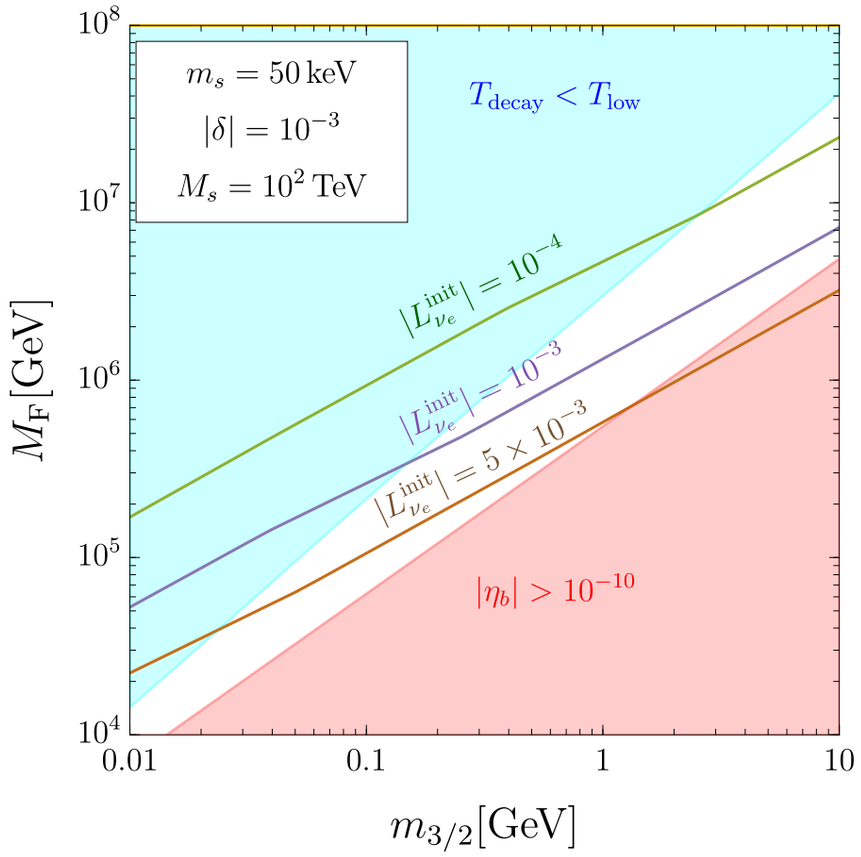

3. Observational implications

Enhancement of second-order scalar-induced gravitational waves at Q-ball decay

In our model, Q-balls can dominate over the energy density of the universe before the decay.

K. Inomata et al. (2019)
M. Kawasaki, K. Murai (2023)

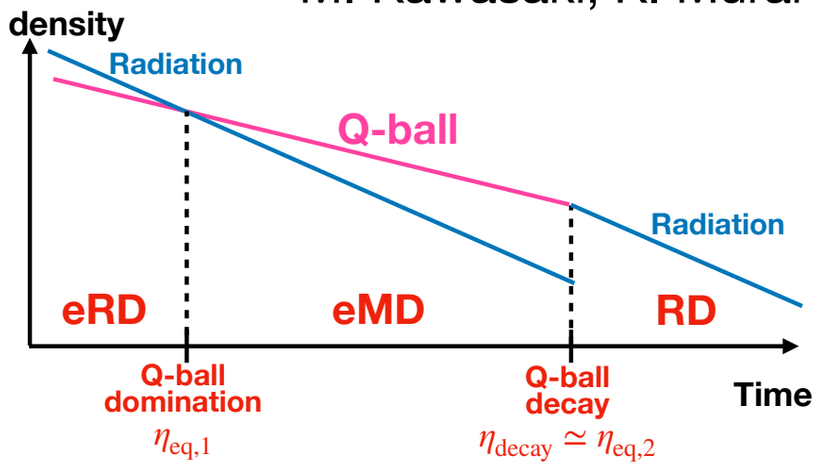

- Energy of Q-balls

$$\Gamma \equiv -\frac{1}{Q}\frac{\mathrm{d}Q}{\mathrm{d}t} = \frac{4}{5}\frac{1}{t_{\rm dec}-t},$$

$$M_{\rm Q} = M_{\rm Q}(0)\left(1-\frac{t}{t_{\rm dec}}\right)^{3/5}$$

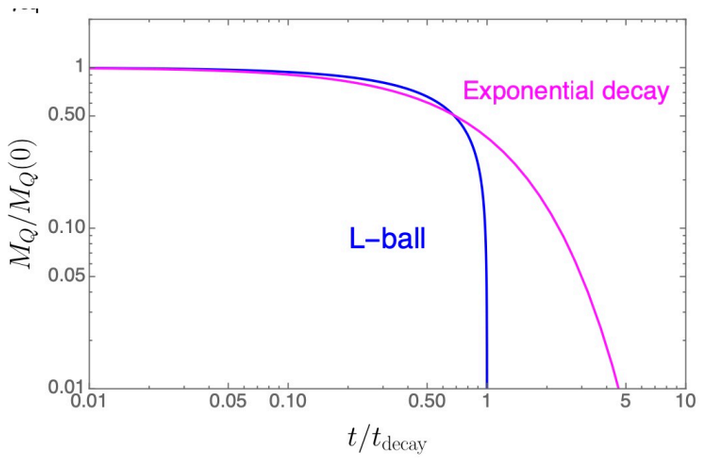

- Time evolution of Φ

The amplitudes do not have sufficient time to decay right before the oscillation

→ The **large amplitude of oscillation lead to the GW production** through <u>second-order effect</u>

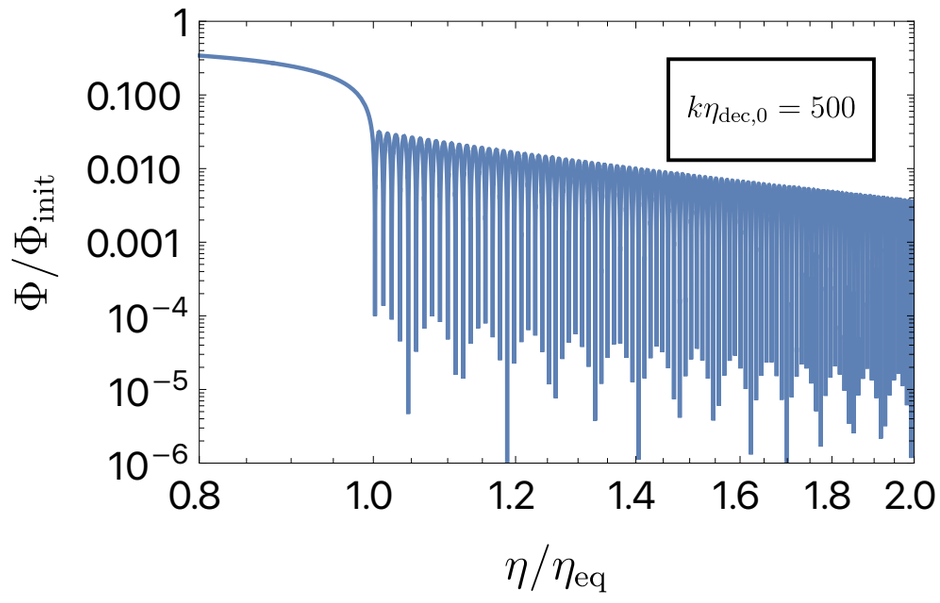

Enhancement of second-order scalar-induced gravitational waves at Q-ball decay

- **Scalar-induced gravitational wave** D. Bauman et al. (2007)

Take conformal-Newtonian gauge :

$$\mathrm{d}s^2 = a^2(\eta)\left[-\left(1+2\Phi^{(1)}+2\Phi^{(2)}\right)+2V_i^{(2)}\mathrm{d}\eta\mathrm{d}x^i+\left[\left(1-2\Phi^{(1)}-2\Phi^{(2)}\right)\delta_{ij}+\frac{1}{2}h_{ij}\right]\mathrm{d}x^i\mathrm{d}x^j\right]$$

Second-order perturbation of Einstein tensor and stress tensor:

$$G_j^{(2)i} = \frac{1}{4}a^{-2}(h_j''^{(2)i}+2\mathcal{H}h_j'^{(2)i}-\Delta h_j^{(2)i})+(\text{second order terms with respect to }\Phi_{,i})$$

$$T_j^{(2)i} \supset \left(\rho^{(0)}+P^{(0)}\right)v^{(1)i}v_j^{(1)}$$

EOM for second-order GW:

$$\leftrightarrow h_{ij}''^{(2)}+2\mathcal{H}h_{ij}'^{(2)}-\Delta h_{ij}^{(2)} = -4\hat{\mathcal{T}}_{ij}^{lm}S_{lm},$$

where $S_{lm} \equiv 3(1+c_s^2)\mathcal{H}^2 v_l^{(1)}v_m^{(1)}+(\text{second order terms with respect to }\Phi)$

Since $v_i^{(1)} = \dfrac{-2\mathcal{H}\Phi_{,i}^{(1)}-2\Phi_{,i}'^{(1)}}{(1+c_s^2)\mathcal{H}^2},$

$$h''^{(2)}+2\mathcal{H}h'^{(2)}-\Delta h^{(2)} = \mathcal{O}(\Phi^2)$$

Second order GW can be induced by time derivative of Φ

Enhancement of second-order scalar-induced gravitational waves at Q-ball decay

We consider the time evolution of Φ before and after Q-balls decay and estimate the resultant GW spectrum

- During eMD :

  At linear level, Φ is conserved

  However, the small-scale density perturbations grows to non-linear

  →Use the result of N-body simulations of density perturbations in MD era, and relate them to Φ by Poisson eq.

$$\delta^2_{\mathrm{m,NL}}(k_{\mathrm{NL}}) = f_{\mathrm{NL}}[\delta^2_{\mathrm{m,L}}(k_{\mathrm{L}})],$$

$$k_{\mathrm{L}} = [1+\delta^2_{\mathrm{m,NL}}(k_{\mathrm{NL}})]^{-1/3} k_{\mathrm{NL}}$$

Poisson eq : $k^2_{\mathrm{NL}}\Phi = \mathcal{H}^2 \delta_{\mathrm{m,NL}}(k_{\mathrm{NL}})$

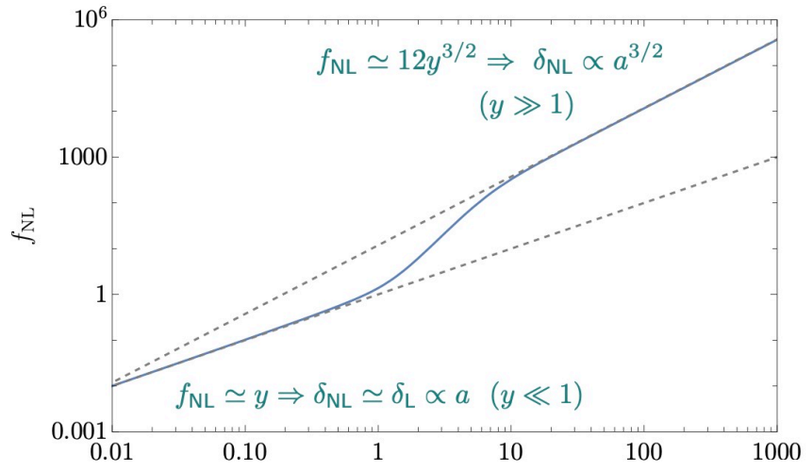

- Transition period :

  When $3a^2|\ddot{\Phi}| \ll k^2\Phi$, Φ decays proportional to M_{Q}

  After that, Φ begins to oscillate satisfying

$$\Phi'' + 4\mathcal{H}\Phi' + \frac{k^2}{3}\Phi = 0$$

Enhancement of second-order scalar-induced gravitational waves at Q-ball decay

KK, K. Murai, M. Kawasaki, 2402.11902

We estimate the gravitational wave spectrum assuming initial flat curvature power spectrum $P_\zeta(k) = C^2 A_s$ ($A_s = 2.1 \times 10^{-9}$) with scale smaller than CMB scale.

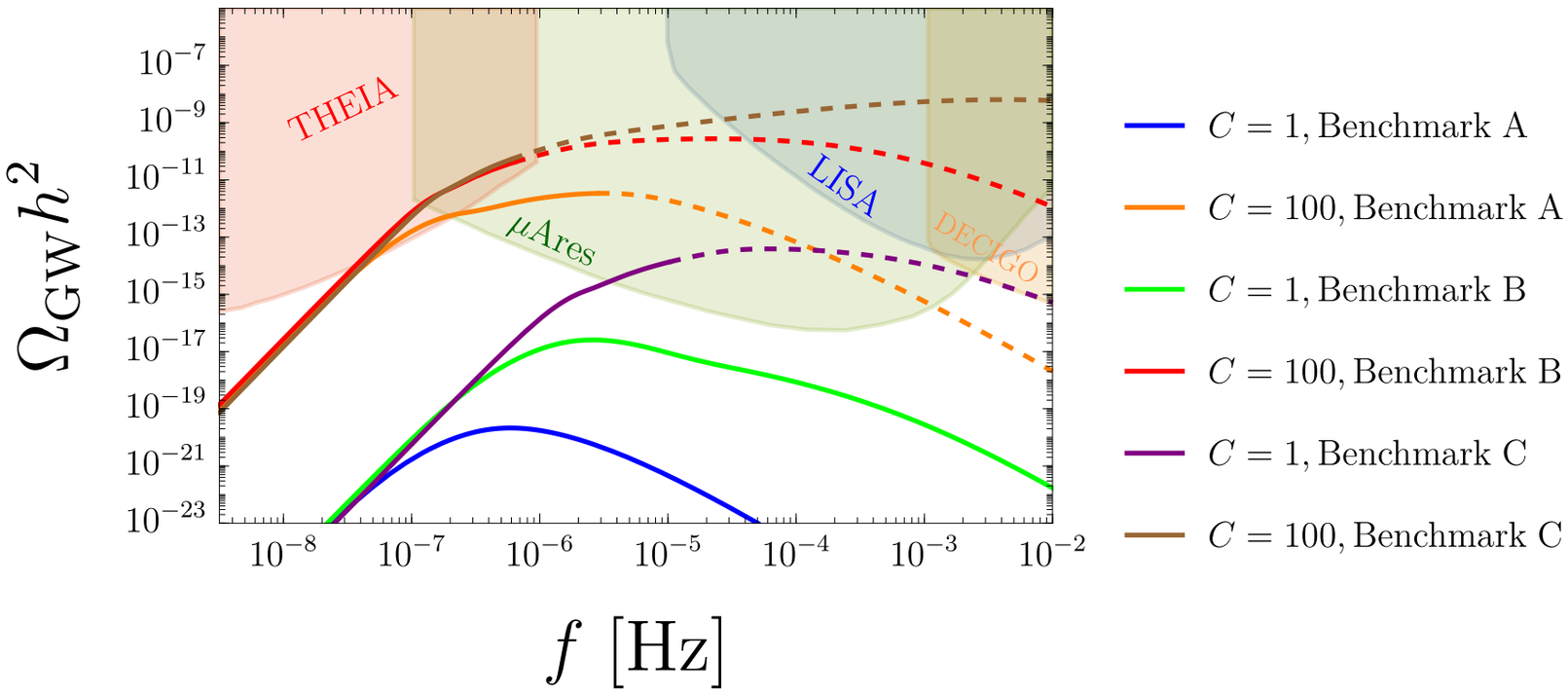

	$m_{3/2}$ [GeV]	$M_{\rm F}$ [GeV]	$T_{\rm R}$ [GeV]	M_s [GeV]	$\lvert\eta_{\rm b}\rvert$	$\lvert L_{\nu_e}^{\rm init}\rvert$
A	0.5	1.3×10^6	1.0×10^2	1.7×10^4	8.7×10^{-11}	4.0×10^{-4}
B	0.4	1.0×10^6	1.0×10^3	2.0×10^5	8.7×10^{-11}	4.8×10^{-4}
C	1.0	2.9×10^6	1.5×10^4	6.6×10^5	8.7×10^{-11}	2.2×10^{-4}

Discussions : Beyond the monochromatic approximation of the Q-ball mass distribution

The mass distribution of the Q-balls have finite width

There will be a cut-off of Q-ball size because they cannot be formed in super-horizon scale at the formation

S. Kasuya, M. Kawasaki, (2002)

→We model the charge distribution of Q-balls as

$$\frac{\mathrm{d}E}{\mathrm{d}\ln Q} \propto Q^{1/\sigma}\Theta(Q_{max}-Q)$$

→Due to the finite σ, the eMD-RD transition becomes more gradual

→The oscillation amplitude of ϕ gets more suppressed

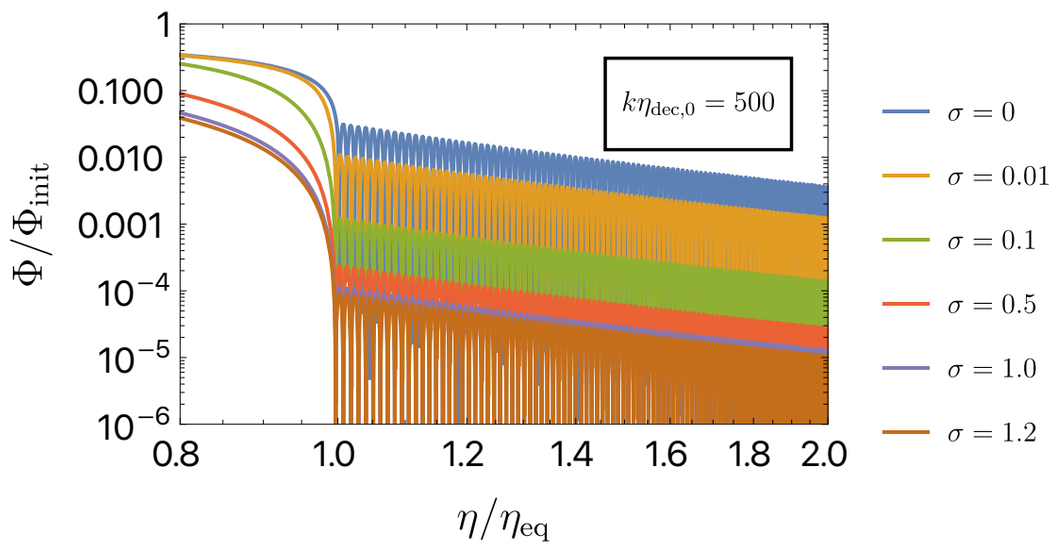

→This suppression becomes strong in the high-frequency region

→will alter the GW spectrum in high k

Conclusion

1. We revisited the calculation of resonant production scenario of sterile neutrino DM and confirmed that initial lepton asymmetry is required to be $L_e \gtrsim \mathcal{O}(10^{-4})$ and $m_s \gtrsim 10$ keV to evade the current X-ray constraints.

2. We showed that Affleck-Dine leptogenesis can successfully be consistent with Shi-Fuller mechanism.

3. We estimated the power spectrum of background GW from Q-ball decay effect and showed that this scenario can be tested by future LISA/DECIGO/μAres/THEIA experiment.